A Novel Time-Series Database of Finger Hypercubes Before and After Hand Sanitization with Demographics

Sriram Sai Sumanth(✉) and Emanuela Marasco

Center for Secure Information Systems, George Mason University,
Fairfax, VA 22030, USA
{ssriram2,emarasco}@gmu.edu

Abstract. During the past decade, hyperspectral imaging (HSI) has been an area of broad, innovative work in a variety of applications such as health, defense, and remote sensing. Hyperspectral images can be collected using a compact HSI imager and are referred to also as hypercubes. Currently, there are no biometric hyperspectral databases available to the community. In this paper, we create the Finger Hypercubes Sanitization with Demographics Database (FHSD) (https://github.com/cysber-CSIS/GMU-CSIS—Finger-Hypercubes-Sanitization-with-Demographics-FHSD-2022) consisting of hyperspectral images of human fingers along with their demographics (*i.e.*, age, gender, and ethnicity) captured before and after hand sanitization. This gender-balanced database consists of images pertaining to 100 subjects collected in an indoor environment with a white background under proper lighting conditions using the Resonon bench-top Pika-L hyperspectral imaging system (400–1000 nm). For each subject, multiple left and right index samples were acquired before and after sanitization. In addition to spatial information, HSI data provides 281 channels decoding a spectral component able to describe skin reflectance. Thus, this data holds great potential for enabling a more in-depth analysis of demographic differentials in fingerprints compared to conventional sensing technologies.

Keywords: Hyperspectral Imaging · Hypercubes

1 Introduction

Despite several benefits, the use of algorithmic decision systems is also associated with different risks for individuals, such as discrimination and unfair practices. In particular, biometric systems (*e.g.*, face and fingerprint recognition) have exhibited undesirable demographic differentials by yielding lower genuine scores for ethnic minorities and women. While numerous studies evaluate the fairness of various face recognition systems, these studies are limited for fingerprint recognition [15]. Over the past decade, researchers have demonstrated the possibility of predicting gender from fingerprint images. The majority of current methods for predicting gender rely on techniques based on textural properties such as ridge density [2,15].

J.-J. Rousseau and B. Kapralos (Eds.): ICPR 2022 Workshops, LNCS 13645, pp. 597–609, 2023.
https://doi.org/10.1007/978-3-031-37731-0_43

Over the past ten years, sensor-based fingerprint recognition systems have been under careful examination to see if they exert racial and gender bias. It has been found that the use of Binarized Statistical Image Features (BSIF), Local Binary Patterns (LBP), and Local Phase Quantization (LPQ) were able to identify features to discriminate males from females fingerprint images with an accuracy of 88.7% using K-Nearest Neighbor. To further explore gender classification with respect to capture bias, cross-sensor evaluation was performed using local textural descriptors (LBP, and BSIF) achie-ved an accuracy of 80% [2,15].

Recent studies found that demographic covariates may exhibit bias in fingerprint match scores obtained using automatic matchers. ROC regression techniques have been used to evaluate the impact of demographics such as age, gender, and ethnicity on the performance of the latent fingerprint automatic matchers. These techniques show that the models perform significantly better on male subjects with an AUC of 71% and 76% for the right index and thumb instances respectively. They perform even better when latent image quality has been used as an auxiliary covariate along with the demographics [4,18,19]. Statistical testing frameworks have also been used to evaluate biases in a commercial-off-the-shelf fingerprint matcher (VeriFinger 12.3 SDK) and a neural fingerprint matcher (DeepPrint). The highest True Match Rate (TMR) was observed in females with a TMR of 99.58% and 93.3% for Verfinger 12.3 and DeepPrint, respectively. The analysis of biases in fingerprints may be limited by existing sensing technologies; therefore, we propose to investigate the problem from a richer perspective, i.e., in the hyperspectral domain [1,3,5].

Over the past few years, Hyperspectral imaging (HSI) has been used across various fields such as forensic science, seed viability, environmental monitoring, and food quality checks [12]. Recently, HSI has also gained a lot of interest in biometrics and is used to analyze a person's physical and biological characteristics to authenticate and verify their identity [7–11]. These imagers collect both spectral and spatial information from the subjects and hence are more widely adopted by many security services to expand their capabilities for different biometric purposes. HSI can measure continuous spectral bands to analyze a wide spectrum of light instead of assigning primary colors (red, green, and blue) to each pixel. While a standard RGB camera acquires data across 3 channels, the hyperspectral imager collects data from 281 channels and offers a much wider spectrum. It uses fine wavelength resolution to measure the continuous spectrum of light for each pixel of the scene, not only in the visible but also in the near-infrared region [14]. Using deep learning technology in HSI analysis has advanced quickly in recent years and attracted a lot of attention. Researches have been conducted to develop deep learning models for hyperspectral image classification specifically to deal with a few labeled samples by proposing techniques to achieve good performance in such a critical scenario including autoencoders, few-shot learning, transfer learning, activate learning, and data augmentation [37].

In this paper, we create the Finger Hypercubes Sanitization with Demographics (FHSD) database which is the first one providing containing finger hypercubes from 100 subjects with demographics. The images are captured in various temporal sessions, *i.e.*, before and after applying hand sanitizer, enabling the analysis of the impact of this

product on the spectral signature of finger data. The collection is multi-instance (*i.e.*, left and right index) and multi-sample (*i.e.*, three per subject).

The rest of the paper is structured as follows: Sect. 2 describes recent applications of hyperspectral technology. Section 3 presents technical details about HSI scanning methods and acquisition modes. Section 4 discusses the data collection protocol, the tools used, and the challenges faced, and Sect. 5 draws our conclusion.

2 Literature Review

Lately, subject identification and authentication using hyperspectral and multispectral imaging have gained a lot of interest due to their ability to collect spectral information from the subjects besides spatial information by acquiring their data cubes from across the different bands of the electromagnetic spectrum.

In 2008, Robila proposed an approach to study and analyze the efficiency of hyperspectral face recognition and the effectiveness of human matching based on spectral characteristics by acquiring the data in indoor and outdoor environments from over 120 bands across multiple spectra in various angles. It was performed to improve the face recognition by combining images from different sources, such as the visible and the infrared spectrum. They observed that spectral angle and data together could be used to differentiate humans [9].

In 2017, L. Di Cecilia *et al.* built an optical system and developed a method to measure the spectral reflectance of the human iris. They collected data in the spectral range of 440 to 900 nm. By performing hyperspectral analysis on the iris, its pigmentation and age-related changes could be observed over time. They also found that machine learning techniques like k-means clustering can be used to improve the evaluation of iris structural features [10]. In 2017, Dabhade *et al.* conducted a laboratory experiment to perform an analysis on human authentication using a hyperspectral face database of 120 cubes collected from 70 subjects. They performed feature extraction on the UWA HSFD database developed by the university of Western Australia using principal component analysis. They found that recognition rates of hyperspectral face images vary across different spectral bands [11].

In 2018, Jenerowicz *et al.* conducted a study to analyze the possibilities of using a pushbroom hyperspectral camera to interpret the hand biometric characteristics, such as hand shape and vein pattern of the subjects, for accurate identification. They found that data collected at 900mm (near-infrared region) could be used to better identify the hand's vascular patterns, making it a viable alternative to currently available commercial biometric systems [8].

In 2022, Marasco *et al.* conducted a study to analyze the impact of hand sanitizer on the spectral signature pertain to finger hypercubes using a subset of the proposed Finger Hypercubes Sanitization with Demographics (FHSD) database. They built a framework to perform a non-parametric classifier-based two-sample test to determine whether the spectral signals collected from the finger hypercubes before hand sanitization differs from the signal collected after hand sanitization. They found that hand sanitizer does not have a significant impact on the finger hypercubes [6].

3 Fingerprints in the Hyperspectral Domain

Electromagnetic radiation (EMR) is energy in the form of electromagnetic waves that interact with substances in various ways depending on whether it strikes a solid, liquid, or gas and undergoes one or more of the processes of reflection, absorption, and transmission. Reflection occurs when the electromagnetic radiation is reflected by the target surface upon which it is incident. The absorption process, on the other hand, occurs when the target absorbs the incident radiation. Finally, transmission occurs when the radiation passes through the target unaffected [27–30]. The physical characteristics of the target and the wavelength of the incident light determine how much light is absorbed, reflected (which the camera can capture), and transmitted by the target.

Light is an EMR within a visible region that enters human biological tissue, which undergoes multiple scattering and absorption events as it travels through it. The analeptic window spanning from 600 to 1300 nm allows significant light penetration because most tissues are weak absorbers. The penetration depth of light entering the human biological tissues is determined by the tissue's ability to absorb it [32]. This light absorbed is either converted to heat or is radiated in the form of luminescence. The EMR in this visible to the near-infrared region can penetrate the skin up to 4–5 mm [33]. Over time, long exposure of the instrument to the light will lead to accumulation of electrons, leading to dark currents, *i.e.*, a flow of charges in the absence of light. This phenomenon generates noise in the hypercubes which must be eliminated by dark current correction [31,43].

HSI systems are categorized based on the acquisition mode and on how the target's spectral and spatial information is obtained [34]. There are two main types of scanning methods: spatial (point and line) and spectral (area) scanning [35], and three ways to acquire the hypercube: point, line, and area scanning [36].

As shown in Fig. 1, point scanning (also known as whisk-broom imaging) is the most time-consuming method in which the spectrum is procured at only one spatial location at a time, and then the detector or the target is moved to acquire other points. It aids in obtaining a high spectral resolution to perform a more detailed analysis of the captured pixel [38].

Pushbroom cameras (also known as Line-scan cameras) can scan 100 times faster than point-scan cameras while still achieving high spectral resolution, see Fig. 1 [39, 40]. At a given time, the imager captures one line of pixels from the target (y-axis). Moving the camera's field-of-view (FOV) in that direction generates the other spatial dimension (x-axis) [38].

Area scan (also known as staring imaging) acquires the hyperspectral image one wavelength at a time from the target using a rotating filter or a tunable filter such as LCTF or AOTF, as shown in Fig. 1. This method requires no relative movement between the target and the imager, and the imager captures a whole spatial scene (wavelength) at each spectral band in a sequence [41]. Hyperspectral images are a stack of images collected across the electromagnetic spectrum by obtaining a continuous spectrum of wavelengths for every pixel in an image. The images are collected at different spectral bands resulting in three-dimensional data structures containing two spatial dimensions (X-Y) and one spectral dimension (λ) known as a hypercube [42]. The Resonon Pika L line scan camera was used to collect the hypercubes in this study. As the object is

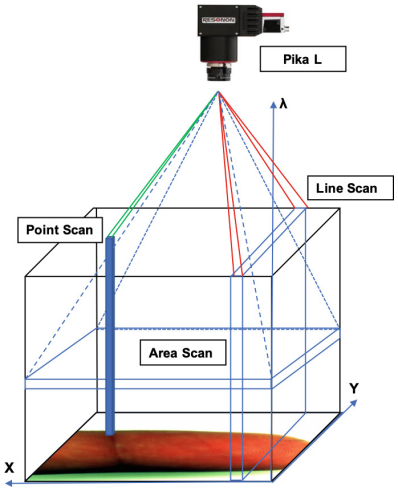

Fig. 1. Classification of different types (line, point, and area scan) of hyperspectral cameras and the amount of data each camera acquires within a single scan.

translated, it gathers data one line at a time and assembles multiple lines to complete the two-dimensional image; this line-by-line assembly of the numerous line-images results in a complete finger hypercube with spectral and spatial dimensions. The application of this system can be extended and used to distinguish demographic information such as age and gender and can also perform contactless fingerprint recognition using machine learning. As this imager collects the data across 281 spectral channels, it helps analyze the biochemical content in the finger skin for a better understanding of the effect of hand sanitizer on spectral information across the subjects over time. Therefore, our database bridges the gap between biometrics and advanced image processing, making it distinct from other databases in the biometric community.

4 The Data Collection

The hypercubes and the demographics were collected from 100 subjects. The subjects are gender-balanced, as shown in Fig. 2, and are primarily students, their families, and friends who are 18 years of age or older, free of metabolic diseases, malfunction of the genetic disorder of metabolism (e.g., diabetes), and are of normal weight. We collected data from people of various ages and backgrounds. In terms of ethnicity, 84% of the subjects are Asians/Asian Americans, 6% are Hispanic/Latino, 6% are White/Caucasians, and 4% are North African/African Americans. The subjects with known health issues and under any kind of hormone treatment are excluded from this study. Individuals with open wounds/cuts on their hands were also excluded due to the burning sensation caused by the hand sanitizer.

For each subject, six hypercubes (3 per finger) were collected from the left and right index fingers before the hand sanitizer was applied, as shown in Fig. 3. Once the hand

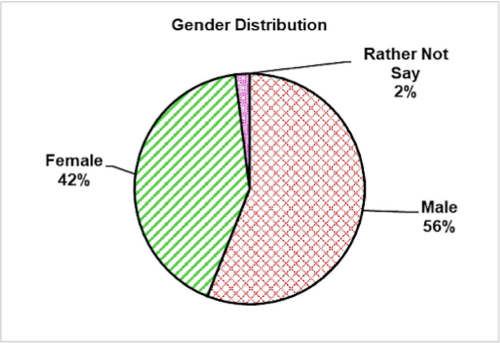

Fig. 2. Distribution of gender for the participants of the data collection.

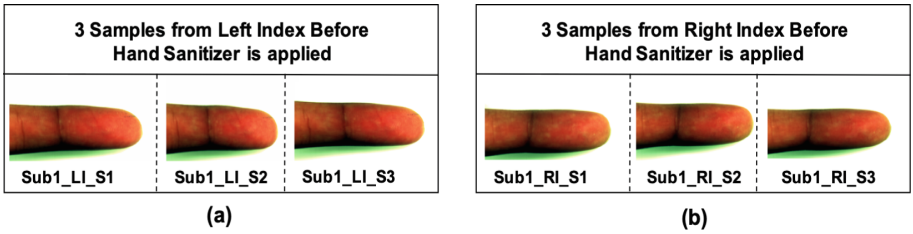

Fig. 3. Hypercube samples collected before hand sanitization: (a) Hypercubes captured from the left index before hand sanitization, and (b) hypercubes captured from the right index before hand sanitization.

sanitizer is applied, each fingerprint instance was collected three times after 1, 10, and 25 min resulting in a total of 24 hypercubes collected from each subject as shown in Fig. 4. In total this dataset comprises of 600 hypercubes collected before sanitization and 1800 hypercubes from both the fingers after hand sanitization as shown in Table 1. Therefore, it comprises a total of 2400 hypercubes collected from 100 subjects, and the total time taken for each subject during the data acquisition is 45 min. In this data collection, each finger hypercube at an instance is collected three times to better understand the spectral variations at each instance. To study demographic biases, the demographic data were also collected from the subjects via an in-person paper survey. For this collection, we used Purell hand sanitizer containing 70% ethanol, manufactured by GOJO, and subjects applied a single pump of hand sanitizer, approximately 3 ml of this product once the six hypercubes were collected before hand sanitization.

The challenges encountered during this data collection involve difficulties for some of the subjects in placing their finger directly under the camera, others faced problem to keep their finger still while the stage was moving. Some of the subjects could not look and put their finger directly under the camera due to the halogen lighting assembly being too bright. A few technical challenges faced during the initial assembly of the bench-top system are setting the stage controls and focusing the objective lens of the imager. As Pika-L is a line scan camera, the stage must move at a speed proportional to

Table 1. Details about the data collected in this study.

Sanitization	# of Subjects	Finger instance	Time (min.)	# of Samples per Subject	# of Datacubes
Before Sanitization	100	Left Index	0	3	300
		Right Index		3	300
After Sanitization		Left Index	1	3	300
			10	3	300
			25	3	300
		Right Index	1	3	300
			10	3	300
			25	3	300
				Total # of Datacubes	2400

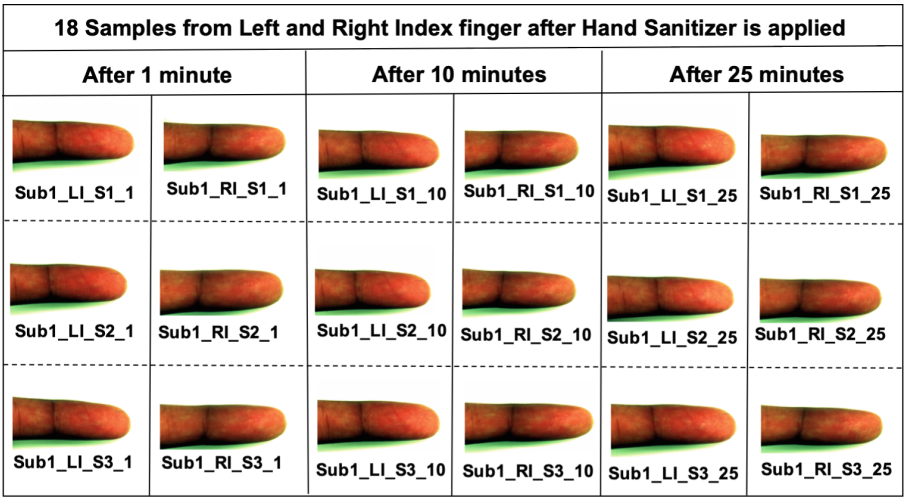

Fig. 4. The 18 hypercubes, 6 collected at each instance from the left (L) and right (R) index fingers after 1, 10 and 25 min of hand sanitization.

the imager's frame rate to acquire the target with a unit aspect ratio. The image could be elongated or shortened if the stage is too slow or too fast in comparison to the frame rate of the camera. Focusing the bench-top system's objective lens is a difficult task that is accomplished by placing a calibration sheet within the imager's field of view and rotating the lens with an allen wrench until the sheet is focused.

4.1 The Sensing Module

The data was captured by using the Resonon bench-top hyperspectral camera Pika L illustrated in Fig. 6. The resonon bench-top system comprises of a linear translation stage, mounting tower, lighting assembly, and SpectrononPro software installed

on a desktop computer. The Pika L is a lightweight and compact Visible Near Infrared (VNIR) hyperspectral imager with a maximum frame rate of 165fps; it has a 23 mm lens with a spectral range of 400–1000 nm, as shown in Fig. 5, 281 spectral channels, 13.1° field of view, 2.1 nm spectral resolution, and 900 spatial pixels. The Resonon Hyperspectral cameras are line scan imagers that collect data one line at a time. The multiple line images are then pieced together line-by-line to form a final image. A linear stage assembly is used in the bench-top system, which is moved forward and backward with the help of a stage motor [43].

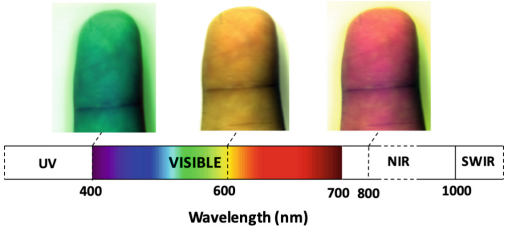

Fig. 5. Finger hypercubes across the Electromagnetic spectrum

The pika imaging spectrometers were connected to the computer via USB cables; one of the two USB ports was connected to the camera, which supplies power to the camera; the second USB (Black) port from the computer was connected to the stage of the bench-top system via the Mini USB connection, and the DC power supply powers the stage. Finally, another regulated power supply was used to supply power to the lighting assembly of the bench-top system [43].

Four halogen bulbs are positioned above the stage to emit light at a proper angle to focus the scene and create ideal scanning conditions. Resonon's laboratory bench-top hyperspectral imaging system uses broadband halogen lighting for hyperspectral reflectance measurements. The lights used in the 4-fixture are: 5300 Kelvin 36 Degree 12V 35W Halogen Flood Light Bulb. A stabilized power supply controls these lights, reducing variation caused by illumination fluctuations [43]. Since hyperspectral imaging separates light from a scene into many spectral components, the total radiation incident on a single sensor pixel is relatively small. The halogen lighting assembly provides adequate illumination at all wavelengths to acquire high-quality hyperspectral data from the bench-top system. The hyperspectral imaging system was set up with a distance of about 25 cm between the lens and the linear stage, with the lighting assembly also at the same level as the lens. Once the lighting assembly is adjusted to focus on the linear stage, the dark currents are corrected by blocking all the light entering the lens of the camera with the cap as shown in Fig. 7(a). The camera is then calibrated for response correction by placing a white tile under the lens; these corrections are performed in the same environment where the data collection was performed.

The Spectronon Pro is the software used by Resonon to control its bench-top system. It is connected to the Pika L camera via a USB cable. As shown in Fig. 6(b), this software performs all of the scans and collects hypercubes from each subject. Before

performing the scans, the camera and stage parameters of the bench-top system are adjusted using the Spectronon Pro interface. It analyzes the hypercube across various wavelengths by selecting the Region of Interest (ROI) and generating the mean spectrum for each ROI in the hypercube.

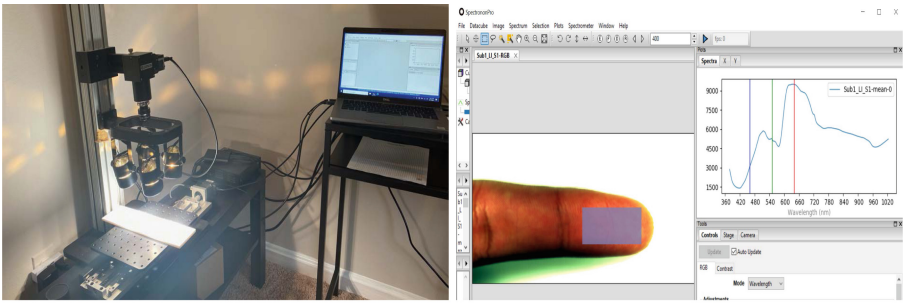

(a) (b)

Fig. 6. The Resonon bench-top system: (a) the hyperspectral camera Pika L, and (b) the spectronon Pro interface used to collect the hypercubes from the subjects.

4.2 The Protocol

Data from each subject is collected by placing the subject's left and right index fingers under the camera. As shown in Fig. 3(a) & Fig. 3(b), each fingerprint instance is collected three times using the HSI camera before the hand sanitizer is applied. Once the hand sanitizer is applied, each fingerprint instance is collected three times after 1, 10, and 25 min as shown in Fig. 4. These images are equally distributed over both genders and are stipulated with their respective demographics. Before starting the acquisition, a white tile is placed under the camera to provide a white background while capturing the image and it is placed three holes from the right. The finger should be placed 1 cm from the border of the white surface in a way that the finger is under the camera, as shown in Fig. 7(b).

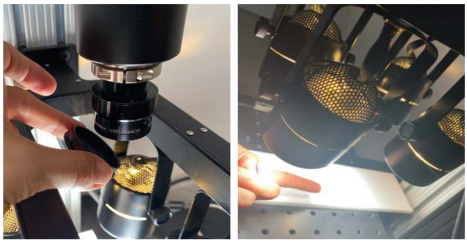

(a) (b)

Fig. 7. (a) Dark current correction by blocking the lens (b) Placing the finger on the white surface for hypercube acquisition.

To acquire the hypercubes, subjects are asked to perform the following steps,

- The subjects are first asked to place their left index finger on the white surface under the camera without moving it, and three hypercubes are collected.
- The subjects then place their right index finger under the camera and three more hypercubes are collected before the hand sanitizer is applied.
- After applying the hand sanitizer, 6 hypercubes are collected, 3 at each instance from the left and right index fingers after 1, 10, and 25 min, resulting in a total of 18 hypercubes after the hand sanitization.

The hypercubes are saved in .bil format. The nomenclature of the hypercubes collected before sanitization is shown in Fig. 8(a). The first four digits indicate the subject's label, which ranges from 1 to 100. The two characters after the underscore denote if the hypercube is collected from the L (left) or R (right) index finger. Finally, the sample number, which ranges from S1 to S3, is indicated by the last two characters after the underscore. Hypercubes collected after sanitization are labeled similarly, with the exception that the time after which the hypercubes were collected is stated last after the underscore, as shown in Fig. 8(b).

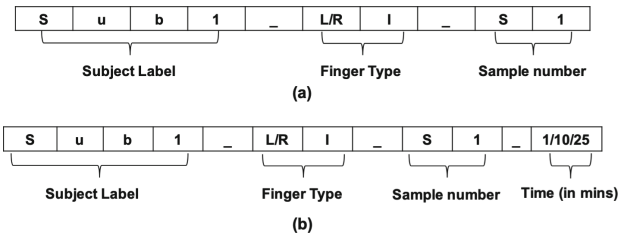

Fig. 8. (a) Nomenclature for the hypercubes collected before hand sanitization, (b) Nomenclature for the hypercubes collected after hand sanitization.

5 Conclusions

This paper presents a new biometric database of hyperspectral images of fingers pertaining to 100 subjects along with their demographics (age, gender, and ethnicity) from left and right index. Furthermore, the images were captured before and after 1, 10, and 25 min of applying a hand sanitizer. For each subject, three samples per finger were collected to study intra-class variability. The data acquisition protocol was carefully designed to minimize changes of biochemical content in finger skin reflectance and subsequently in the spectral signature. Participants with metabolic diseases and genetic disorders were not eligible to minimize variations in the spectra. Calibration and setup procedures pertaining to the instrument Resonon Pika L hyperspectral imager used in this data collection are also described.

In future work, we will: *i)* extend the experiments by considering additional commercial hand sanitizer to study how they affect the spectral and spatial features, *ii)*,

design algorithms for HSI gender and age estimation to understand and mitigate demographic differential in fingerprint data, and *iii)* establish a benchmark that evaluates the robustness of spectral signature with respective hand sanitization.

Acknowledgment. This work was funded by the National Science Foundation (NSF) grant #2036151.

References

1. Marasco, E.: Biases in fingerprint recognition systems: where are we at? In: 2019 IEEE 10th International Conference on Biometrics Theory, Applications and Systems (BTAS), pp. 1–5 (2019)
2. Marasco, E., Lugini, L., Cukic, B.: Exploiting quality and texture features to estimate age and gender from fingerprints. In: Biometric and Surveillance Technology for Human and Activity Identification XI, vol. 9075, pp. 112–121. SPIE (2014)
3. Jain, A.K., Deb, D., Engelsma, J.J.: Biometrics: trust, but verify. arXiv preprint arXiv:2105.06625 (2021)
4. Marasco, E., He, M., Tang, L., Tao, Y.: Demographic effects in latent fingerprint matching and their relation to image quality. In: 2022 7th International Conference on Machine Learning Technologies (ICMLT), pp. 170–179 (2022)
5. Godbole, A., Grosz, S.A., Nandakumar, K., Jain, A.K.: On demographic bias in fingerprint recognition, arXiv preprint arXiv:2205.09318 (2022)
6. Marasco, E., Tao, Y.: Mitigating the impact of hand sanitizer on the spectral signature of finger hypercubes. In: 2022 International Joint Conference on Biometrics (IJCB 2022) (2022)
7. Roui-Abidi, B., Abidi, M.: Multispectral and Hyperspectral Biometrics. In: Li, S.Z., Jain, A. (eds.) Encyclopedia of Biometrics, pp. 993–998. Springer, Boston (2009). https://doi.org/10.1007/978-0-387-73003-5_163
8. Jenerowicz, A., Walczykowski, P., Gladysz, L., Gralewicz, M.: Application of hyperspectral imaging in hand biometrics, vol. 10802, p. 108020G (2018)
9. Robila, S.A.: Toward hyperspectral face recognition. In: Image Processing: Algorithms and Systems VI, vol. 6812, pp. 296–304. SPIE (2008)
10. Di Cecilia, L., Marazzi, F., Rovati, L.: Hyperspectral imaging of the human iris, p. 104120R (2017)
11. Dabhade, S.B., Bansod, N., Rode, Y., Kazi, M., Tharewal, S., Kale, K.: Hyper spectral image analysis for human authentication, pp. 1–4 (2017)
12. GringGIS: 10 important applications of hyperspectral image (2016). https://grindgis.com/remote-sensing/10-important-applications-of-hyperspectral-image
13. Rampfesthudson: How does a hyperspectral sensor work? (2019). https://www.rampfesthudson.com/how-does-a-hyperspectral-sensor-work/
14. NIREOS: What is hyperspectral imaging? (2022). https://www.nireos.com/hyperspectral-imaging/
15. Marasco, E., Cando, S., Tang, L., Tabassi, E.: Cross-sensor evaluation of textural descriptors for gender prediction from fingerprints. In: IEEE Winter Applications of Computer Vision Workshops (WACVW), pp. 55–62. IEEE (2019)
16. Rathgeb, C., Drozdowski, P., Frings, D.C., Damer, N., Busch, C.: Demographic fairness in biometric systems: what do the experts say? arXiv preprint arXiv:2105.14844 (2021)
17. Marasco, E.: Biases in fingerprint recognition systems: where are we at? In: 2019 IEEE 10th International Conference on Biometrics Theory, Applications and Systems (BTAS), pp. 1–5. IEEE (2019)

18. Yoon, S., Jain, A.K.: Longitudinal study of fingerprint recognition. Proc. Natl. Acad. Sci. **112**(28), 8555–8560 (2015)
19. Marasco, E., He, M., Tang, L., Sriram, S.: Accounting for demographic differentials in forensic error rate assessment of latent prints via covariate-specific ROC regression. In: Singh, S.K., Roy, P., Raman, B., Nagabhushan, P. (eds.) CVIP 2020. CCIS, vol. 1376, pp. 338–350. Springer, Singapore (2021). https://doi.org/10.1007/978-981-16-1086-8_30
20. Lugini, L., Marasco, E., Cukic, B., Dawson, J.: Removing gender signature from fingerprints. In: 37th International Convention on Information and Communication Technology, Electronics and Microelectronics (MIPRO), pp. 1283–1287. IEEE (2014)
21. Marasco, E., Cukic, B., Shehab, M., Usman, R.: Attack trees for protecting biometric systems against evolving presentation attacks. In: 16th Annual IEEE International Conference on Technologies for Homeland Security (HST) (2017)
22. Marasco, E., Cukic, B.: Privacy protection schemes for fingerprint recognition systems. In: Biometric and Surveillance Technology for Human and Activity Identification XII, vol. 9457, pp. 83–96. SPIE (2015)
23. Marasco, E., Vurity, A.: Fingerphoto presentation attack detection: generalization in smartphones. In: 2021 IEEE International Conference on Big Data (Big Data), pp. 4518–4523. IEEE (2021)
24. Taherkhani, F., Dawson, J., Nasrabadi, N.M.: Deep sparse band selection for hyperspectral face recognition, arXiv preprint arXiv:1908.09630 (2019)
25. Socolinsky, D.A., Wolff, L.B., Neuheisel, J.D., Eveland, C.K.: Illumination invariant face recognition using thermal infrared imagery. In: IEEE Computer Society Conference on Computer Vision and Pattern Recognition, CVPR 2001, vol. 1, pp. I-I (2001)
26. Wikipedia: Hyperspectral imaging (2022). https://en.wikipedia.org/wiki/Hyperspectral_imaging
27. Exelis, an introduction to hyperspectral imaging (2014). https://www.ugpti.org/smartse/research/citations/downloads/Excelis-Introduction_to_HSI_Technology-2014.pdf
28. Government of canada, radiation - target interactions (2015). https://www.nrcan.gc.ca/maps-tools-publications/satellite-imagery-air-photos/remote-sensing-tutorials/introduction/radiation-target-interactions/14637
29. Howard, D.: Electromagnetic radiation absorption (2022). https://study.com/academy/lesson/electromagnetic-radiation-absorption.html
30. College of Earth and Mineral Sciences: The roads traveled most by radiation (2020). https://www.e-education.psu.edu/meteo3/l2_p4.html
31. Thorlabs, P.: Camera Noise and Temperature Tutorial (2020). https://www.thorlabs.com/newgrouppage9.cfm?objectgroup_id=10773#::text=Dark%20Shot%20Noise%20(%CF%83D,excited%20int%20the%20conduction%20band)
32. Vo-Dinh, T.: Biomedical photonics handbook, biomedical diagnostics (2014). https://books.google.com/books?hl=en&lr=&id=IY_LBQAAQBAJ&oi=fnd&pg=PP1&ots=6kuSjbZmyy&sig=zfkgBsD-F5D8Xjnv637xM1IZzlw#v=onepage&q&f=false
33. Wikipedia: Fluorescence (2022). https://en.wikipedia.org/wiki/Fluorescence
34. Kamruzzaman, M., Sun, D.-W.: Introduction to hyperspectral imaging technology. In: Computer Vision Technology for Food Quality Evaluation, pp. 111–139. Elsevier (2016)
35. Lu, G., Fei, B.: Medical hyperspectral imaging: a review. J. Biomed. Opt. **19**(1), 010901 (2014)
36. Qin, J., Chao, K., Kim, M.S., Lu, R., Burks, T.F.: Hyperspectral and multispectral imaging for evaluating food safety and quality. J. Food Eng. **118**(2), 157–171 (2013)
37. Jia, S., Jiang, S., Lin, Z., Li, N., Xu, M., Yu, S.: A survey: deep learning for hyperspectral image classification with few labeled samples. Neurocomputing **448**, 179–204 (2021)

38. Halicek, M., Fabelo, H., Ortega, S., Callico, G.M., Fei, B.: In-vivo and ex-vivo tissue analysis through hyperspectral imaging techniques: revealing the invisible features of cancer. Cancers **11**(6), 756 (2019)
39. Gowen, A.A., Feng, Y., Gaston, E., Valdramidis, V.: Recent applications of hyperspectral imaging in microbiology. Talanta **137**, 43–54 (2015)
40. Liu, Z., Yu, H., MacGregor, J.F.: Standardization of line-scan NIR imaging systems. J. Chemom. J. Chemom. Soc. **21**(3–4), 88–95 (2007)
41. Garini, Y., Young, I.T., McNamara, G.: Spectral imaging: principles and applications. Cytometry Part A J. Int. Soc. Anal. Cytol. **69**(8), 735–747 (2006)
42. Edelman, G.J., Gaston, E., Van Leeuwen, T.G., Cullen, P., Aalders, M.C.: Hyperspectral imaging for non-contact analysis of forensic traces. Forensic Sci. Int. **223**(1–3), 28–39 (2012)
43. Resonon pika l, Bozeman, MT 59715 USA (2014). https://resonon.com/Pika-L